

Warm-Hot Intergalactic Medium in the Sculptor Supercluster

L. Zappacosta,^{1*} R. Maiolino,² F. Mannucci,³ R. Gilli,² P. Schuecker,⁴

¹ *Dipartimento di Astronomia e Scienza dello Spazio, Largo E. Fermi 2, I-50125 Firenze, Italy*

² *Osservatorio Astrofisico di Arcetri Largo E. Fermi 5, I-50125 Firenze, Italy*

³ *Istituto di Radioastronomia - CNR Largo E. Fermi 5, I-50125 Firenze Italy*

⁴ *Max-Planck-Institut für extraterrestrische Physik, Giessenbachstraße, 85748 Garching, Germany*

30 October 2018

ABSTRACT

We have analyzed the soft X-ray emission in a wide area of the Sculptor supercluster by using overlapping ROSAT PSPC pointings. After subtraction of the point sources we have found evidence for extended, diffuse soft X-ray emission. We have investigated the nature of such extended emission through the cross-correlation with the density of galaxies as inferred from the Münster Redshift Survey. In particular we have analyzed the correlation as a function of the temperature of the X-ray emitting gas. We have found a significant correlation of the galaxy distribution only with the softest X-ray emission (0.1–0.3 keV) and only for gas temperatures $kT < 0.5$ keV. We have excluded that this soft X-ray diffuse emission, and its correlation with the galaxy distribution, is significantly contributed by unresolved AGN, group of galaxies or individual galaxies. The most likely explanation is that the soft, diffuse X-ray emission is tracing Warm-Hot Intergalactic Medium, with temperatures below 0.5 keV, associated with the large-scale structures in the Sculptor supercluster.

Key words: Large-scale structure of Universe – X-rays: diffuse background

1 INTRODUCTION

Cosmological simulations predict the formation at low redshifts ($z < 1$) of a diffuse gas phase with temperatures of the order of $T \sim 10^{5.5} \div 10^7$ K and typical densities 10–30 times the mean baryonic density (although 30% of this gas can exceed overdensities greater than 60, and even greater than 100 in the proximity of clusters of galaxies). This gas phase should be distributed in large-scale filamentary structures connecting virialized structures (Cen & Ostriker 1999; Davé et al. 2001). Such Warm-Hot Intergalactic Medium (WHIM) has been identified as the main contributor to the missing matter in the baryonic census, i.e. $\sim 36 \pm 11$ per cent of the baryons (Fukugita & Peebles 2004)¹. The formation of these warm gaseous filaments is due to the infall of baryonic matter onto the previously formed dark matter cosmic web. The gravitational potential of the dark matter heats the gas through shocks and

triggers the formation of galaxies. The WHIM can be observed in the soft X-rays (below ~ 2 keV; Croft et al. 2001) as low surface brightness structures. The detection of its radiation is very difficult because of many Galactic foregrounds (such as the Local Hot Bubble –LHB– and the Galactic halo) and extragalactic background due AGNs, groups of galaxies and clusters. Simulations and X-ray background studies have shown that the WHIM continuum emissivity below 2 keV is roughly of the same order of magnitude as the Galactic foregrounds. More specifically $F_{0.5-2\text{keV}}(\text{WHIM}) \approx 7 \text{ keV s}^{-1} \text{ cm}^{-2} \text{ sr}^{-1} \text{ keV}^{-1}$ (Croft et al. 2001; Kuntz et al. 2001) and $F_{0.2-0.3\text{keV}}(\text{WHIM}) \approx 15 \text{ keV s}^{-1} \text{ cm}^{-2} \text{ sr}^{-1} \text{ keV}^{-1}$ (Croft, private communication). Within this context, Pierre et al. (2000) showed, from simulated observations that *XMM* can observe strong filaments up to $z \sim 0.5$ in the 0.4 – 4 keV energy band.

Cen et al. (1995) pointed out that this gas phase should also emit characteristic spectral lines mainly due to Oxygen, Neon and Iron ions. The level of emissivity of these spectral features is below the sensitivity and spectral resolution limits of the current X-ray instruments. However, cosmological simulations show that these lines will be detectable with the future generation of X-ray satellites (Yoshikawa et al.

* Send offprint requests to: zappacos@nabhas.ps.uci.edu

¹ In this value are comprised both the low redshift Lyman α forest and the OVI absorbers whose independent contribution to the cosmic baryonic fraction is still subject to uncertainties due to the possible double counting of the absorbers, since both phases can coexist in the same systems.

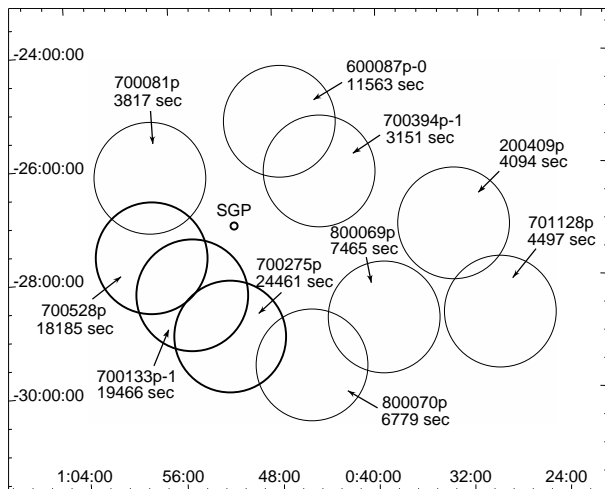


Figure 1. The position of the 10 partially overlapping *ROSAT* PSPC pointings in the region of the SSC. For each pointing the *ROSAT* observation ID and the exposure time are shown. The position of the South Galactic Pole (SGP) is also shown. The three deepest pointings (that will be used for the subsequent quantitative analysis) are identified with thick circles.

2003; Fang et al. 2004).

Various detections of (continuum) WHIM emission have been claimed, either obtained by observing soft X-ray structures in galaxy overdense regions (Scharf et al. 2000; Bagchi et al. 2002; Zappacosta et al. 2002), or by detecting a soft X-ray excess in clusters of galaxies (Kaastra et al. 2003; Finoguenov et al. 2003), or in their proximity (Tittley & Henriksen 2001; Sołtan et al. 2002), or through shadowing effects (Bregman & Irwin 2002). These observations have been possible by means of X-ray satellites very sensitive to low energies ($< 1\text{--}2$ keV), such as *ROSAT* and XMM.

Theoretical works had predicted that the WHIM should be detectable through UV and X-ray absorption lines imprinted on the spectra of background QSOs (Hellsten et al. 1998; Perna & Loeb 1998). The detectability of such absorption features does not depend on the brightness of the filaments but on their column density and on the brightness of the background QSO. So far several detections have been reported through X-ray and far-UV absorption lines probing the hot and cool phase of the WHIM (Nicastro et al. 2002; Tripp 2002; Mathur et al. 2003).

Simulations show that the WHIM should be distributed in filamentary structures extending over several tens of Mpc and connecting clusters of galaxies. Therefore, superclusters (hosting several clusters) are optimal regions where WHIM is more likely to be detected. In this work we focus on the Sculptor supercluster (hereafter SSC, Schuecker & Ott 1991; Seitter 1992). This is one of the richest local superclusters, comprising more than 20 clusters of galaxies (Einasto et al. 1997) spread over a projected length of more than 140 Mpc at a redshift $z \sim 0.105^2$. It is located in the south Galactic pole, a region where the Galactic hydrogen column den-

sity is low enough ($N_H \sim 1.5 \pm 0.2 \times 10^{20} \text{ cm}^{-2}$) to avoid significant effects of patchy absorption that could mimic a pattern of apparent X-ray structures (see Zappacosta et al. 2002, for more details). The SSC has already been observed by Spiekermann (1996) and Obayashi et al. (2000), using *ROSAT* and ASCA data, with the purpose of detecting large-scale X-ray diffuse emission. They did not find indications for emission extended in large-scale structures. However, Spiekermann focused the analysis to the relatively energetic bands at 0.5–3 keV (without investigating the correlation with the galaxy distribution), whereas Obayashi et al. observed in an even harder band (0.8–10 keV) and by using pointings centered on clusters with the goal of detecting hot diffuse emission in their outskirts.

In this paper we present evidence for a correlation between the galaxy distribution and soft X-ray emission in the central region of the SSC. In particular we show that galaxies and the softest X-ray emission (< 0.3 keV) correlate in regions with gas temperatures $kT < 0.5$ keV. This finding is interpreted as WHIM emission associated with the large-scale structures in the SSC.

2 DATA DESCRIPTION

Our aim is to detect the WHIM over the central region of the supercluster ($8.3 \times 6.4 \text{ deg}^2$ corresponding to 57×44 Mpc at $z = 0.105$) which is populated by more than 15 Abell clusters. We considered 10 PSPC partially overlapping pointings taken from the *ROSAT* archive and which cover the core of the SSC (see Fig. 1). Unfortunately, the exposures of these pointings are not homogeneous, ranging from ~ 4 to ~ 24 ksec. As a consequence, our quantitative analysis will be restricted only to the three deepest fields (i.e. those with exposures > 18 ksec, represented with thick circles in Fig. 1).

To map the galaxy density distribution in the SSC we have used data from the Münster Redshift Project (MRSP, Seitter 1992; Spiekermann et al. 1994; Ungruhe et al. 2003). The MRSP is a catalog of galaxies obtained by scanning direct and very low-dispersion objective-prism Schmidt plates over a wide region (5000 deg^2) in the south Galactic hemisphere. We have produced a catalog of all objects identified as galaxies to a limiting magnitude $r_F \sim 20.5^3$. The MRSP catalog is suitable to investigate the SSC just because the photographic plates, where redshifts have been estimated (Ungruhe 1999), efficiently sample objects at redshift $z = 0.1$ (see the redshift histograms in Spiekermann et al. 1994; Ungruhe 1999).

X-ray data have been reduced by using the software described in Snowden et al. (1994), which allows a careful removal of the instrumental background and recovers the effective exposure of each region in the field of view. This careful treatment of the data is optimized to detect faint diffuse structures. Moreover, the high sensitivity below 0.3 keV combined with the large field of view ($\sim 2^\circ$ diameter) make the *ROSAT* PSPC detector the best X-ray instrument to detect diffuse soft structures on large scales (even superior

² Here and in the rest of the paper we will assume a cosmology with $\Omega_m = 0.3$, $\Omega_\Lambda = 0.7$ and $H_0 = 70 \text{ Km s}^{-1} \text{ Mpc}^{-1}$

³ Galactic extinction in this region affects r_F by at most 0.04 magnitudes.

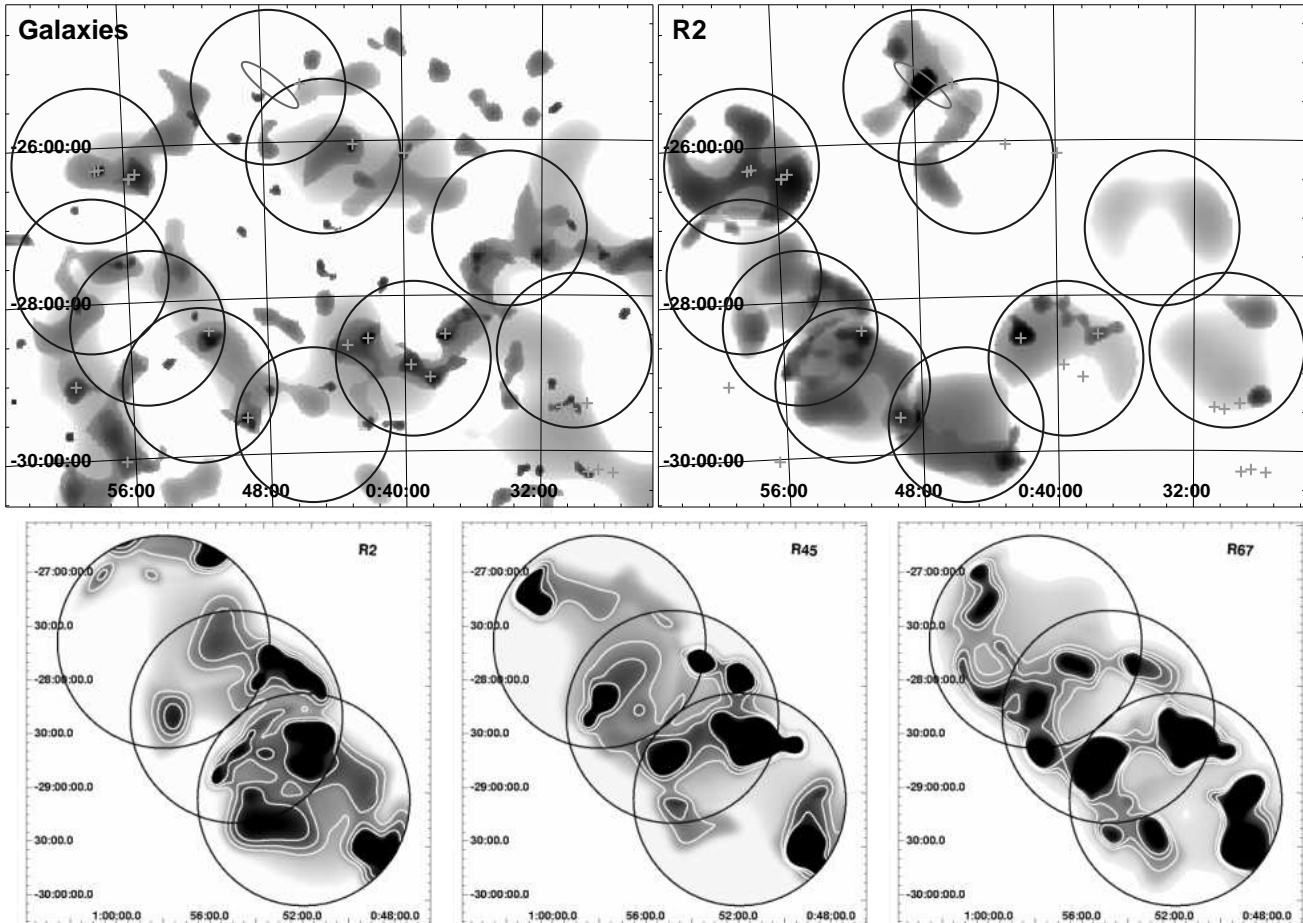


Figure 2. Comparison between structures detected in the distribution of galaxies and in the X-ray *ROSAT* bands. Structures are found with a wavelet algorithm and are significant at 4σ and their extension followed down to 1σ . The top panels show the projected density of galaxies (left) and R2 flux (right) over the whole field covered by the 10 *ROSAT* pointings. Crosses represent clusters members of SSC and the ellipse at the top indicates the location of the large starburst galaxy NGC 253. The bottom panels show (from left to right) the R2, R45 and R67 band maps for the three deepest fields; contours indicate significance levels of 2σ , 3σ and 4σ .

to XMM). We have detected and subtracted point sources (and the few known clusters) from the X-ray image both by using the SExtractor software (Bertin & Arnouts 1996) and by means of a wavelet algorithm (Vikhlinin et al. 1998). The first method identifies point sources in all energy bands by increasing the size of the detection filter as a function of the off-axis angle, to account for the increasing *ROSAT* PSF with off-axis angle. The second method makes use of the wavelet transform to identify structures on various angular sizes. The latter procedure does not account for PSF variations, which were then considered *a posteriori*. The details of both procedures are described in Zappacosta et al. (2002). In the rest of the paper we will use the second method for qualitative considerations and the first one for quantitative analysis.

In order to compare X-ray data with the galaxy catalog we have generated a map of the projected density of galaxies. We have used pixel sizes of $2' \times 2'$ in order to have an average number of galaxies per pixel of about ~ 1 . Moreover, to obtain a better comparison, we have smoothed the galaxy

density images with a gaussian kernel that radially increases like the PSPC PSF.

3 A GLANCE AT THE SCULPTOR REGION

Fig. 2 shows a comparison of the structures found with the wavelet algorithm both in optical and in the three *ROSAT* bands and, more specifically (see also Table 1): 0.14–0.284 keV (R2; the $\frac{1}{4}$ keV band), 0.44–1.21 keV (R45; the $\frac{3}{4}$ keV band), 0.73–2.04 keV (R67; the 1.5 keV band). The upper panels show the projected density of galaxies and the $\frac{1}{4}$ keV flux for all the pointings. The lower panels show the X-ray flux in the three *ROSAT* bands focused onto the region of the three deepest PSPC pointings (see Fig. 1). Contours at significance levels from 2σ to 4σ (spaced by 1σ) are shown in the latter.

Both galaxies and gas show large-scale structures including clusters of galaxies and filamentary structures connecting them. There is also a lot of X-ray diffuse emission not clearly related to visible structures in the galaxy map, which could be due to foreground by our Galaxy (e.g. LHB and

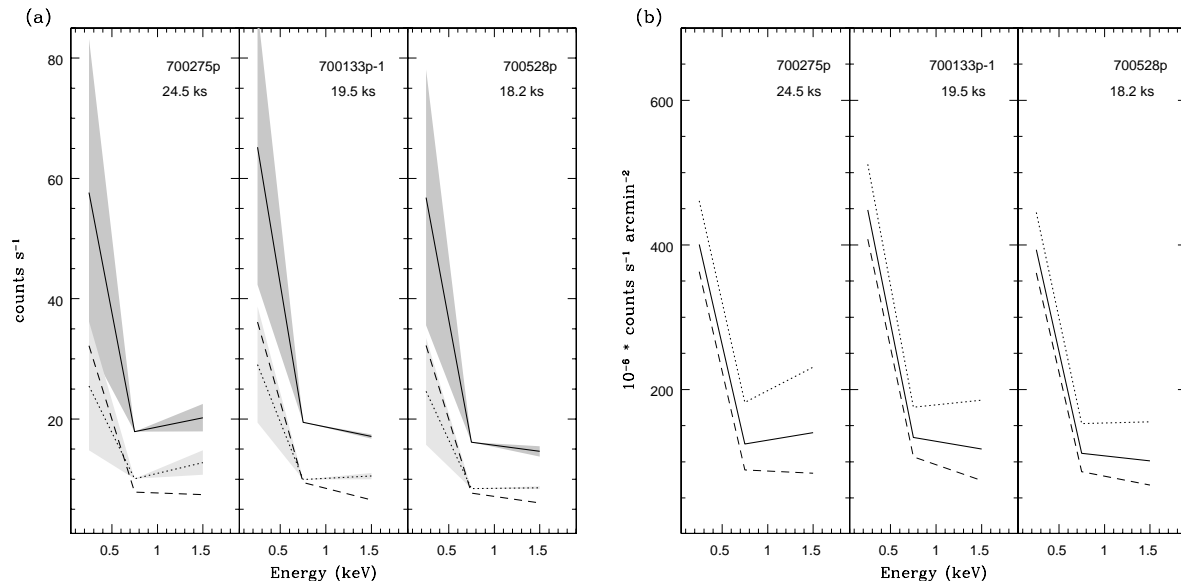


Figure 3. Global spectral shapes (not corrected for Galactic absorption) for the three deepest fields. Panel a): countrate. Panel b): countrate normalized per unit area. The solid lines represent the whole flux detected, the dotted lines show the point sources component and the dashed lines show the residual flux obtained by the subtraction of the first two. Grey regions in panel a) show the dispersions of the spectral shapes over each field.

Table 1. *ROSAT* energy bands and conventional notations.

[b]

Band	Range	Alt. Notation
R2	0.14–0.284 keV	$\frac{1}{4}$ keV ^a
R45	0.44–1.21 keV	$\frac{3}{4}$ keV
R67	0.73–2.04 keV	1.5 keV

^a The notation $\frac{1}{4}$ keV is often referred to the R12 *ROSAT* broad energy band. In the following we will use this notation restricted to the R2 energy band.

Galactic halo) or to a blend of unresolved emission by AGNs (mainly in low exposures pointings). A contribution could also come from foreground (or background) superstructures. Note that Spiekermann (1996) and Obayashi et al. (2000) focused their searches on the harder X-ray emission (i.e. > 0.5 keV) in the region of the *ROSAT* pointing 800069p (see Fig. 1), which is considered the core of the SSC (it contains 5 Abell clusters). This region shows diffuse emission only for the soft $\frac{1}{4}$ keV band (i.e. at energies below 0.3 keV).

4 SPECTRAL ANALYSIS

Filamentary X-ray structures connecting clusters are not necessarily due to warm-hot gas. They could also arise from AGN unresolved emission, as both WHIM and galaxies trace gravitational potential wells of dark matter filaments (Scharf et al. 2000; Zappacosta et al. 2002).

In order to assess the true nature of these filamentary patterns we need to perform an accurate comparison with the

distribution of galaxies along with the analysis of the spectral shape of the X-ray emission. We have to limit our analysis to the three deepest fields (700275p, 700133p-1 and 700528p) where we are confident that a larger fraction of the AGN contribution to the X-ray background has been resolved.

Fig. 3 shows the spectral shapes measured for these pointings sorted by decreasing exposure times. Fig. 3a shows the countrate, while in Fig. 3b the spectra are normalized by the area in each field. Fluxes are not corrected for the Galactic N_{H} absorption (this correction would increase the flux in the $\frac{1}{4}$ keV band by a factor of ~ 3). Dotted lines show the sum of point-like sources detected by SExtractor, while the solid lines show the total flux in each field (shaded regions indicate the dispersions of the slopes within each field). The difference between them is the diffuse residual emission and it is shown with the dashed line. We note that the residual soft, diffuse fluxes have values of $\sim 380 \times 10^{-6} \text{ counts s}^{-1} \text{ arcmin}^{-2}$, well above those found for the LHB emission through shadowing measurements in the region of the south Galactic pole (Snowden et al. 2000), which lie in the range $100 \div 300 \times 10^{-6} \text{ counts s}^{-1} \text{ arcmin}^{-2}$. After subtraction of the LHB and after correction for Galactic absorption, the residual diffuse, extended emission has a value of $\sim 540 \times 10^{-6} \pm 300 \times 10^{-6} \text{ counts s}^{-1} \text{ arcmin}^{-2}$. This residual emission may include both Galactic Halo and extragalactic emission due to either unresolved AGNs, clusters/groups of galaxies and true WHIM emission. We will identify and disentangle these various contributions both through an analysis of the spectral shape and through the correlation with the galaxy distribution.

As discussed above, a residual component due to unresolved AGNs, or unidentified clusters/groups, could still be present even in images with longer exposures. The three

ROSAT energy bands can be used to make a color-color diagram, with the goal of separating colors typical of a warm gas from unresolved AGNs and clusters. In particular, the WHIM is expected to have a softer emission with respect to clusters and AGNs.

Fig. 4 shows the $[\frac{1}{4} \text{ keV}]/[\frac{3}{4} \text{ keV}]$ band ratio (R2/R45) versus the $[\frac{3}{4} \text{ keV}]/[1.5 \text{ keV}]$ band ratio (R45/R67) for different kind of sources (the ratios are in counts and corrected for Galactic absorption). The dotted lines and full symbols indicate the behavior of thermal emission (optically thin plasma, MEKAL model), at a redshift $z = 0.1$ and metallicities of $0.1 Z_{\odot}$ and $0.3 Z_{\odot}$. The dashed lines and hollow symbols indicate colors of AGNs with two different slopes (quite typical in the *ROSAT* band), unabsorbed and with intrinsic absorptions of $N_{\text{H}} = 1 - 5 \times 10^{20} \text{ cm}^{-2}$. The most interesting feature inferred from the color-color diagram in Fig. 4 is that the R45/R67 ratio ($[\frac{3}{4} \text{ keV}]/[1.5 \text{ keV}]$) results to be an excellent tracer of the gas temperature. In particular, gas cooler than $\sim 0.5 \text{ keV}$ (typical of WHIM) is characterized by $R45/R67 > 2$, while gas warmer than 0.5 keV (typical of groups and clusters) or AGNs have $R45/R67 < 2$. Therefore, we have used the ratio R45/R67 to discriminate WHIM regions from areas dominated by unresolved AGNs and clusters.

The X-ray emission in the three fields of the SSC investigated by us spans a wide range of colors. In particular, R45/R67 ranges from ~ 0.5 (typical of AGNs and clusters) to values larger than 2 (typical of WHIM).

5 CORRELATION ANALYSIS

The X-ray colors alone (and in particular the inferred low temperatures) do not necessarily allow the identification of the diffuse X-ray emission with WHIM, since foreground components like LHB and Galactic Halo are also characterized by soft emission and low temperatures. However, any correlation between soft X-ray emission and distribution of galaxies would support the idea that the diffuse X-ray emission is extragalactic and associated with large-scale structures. In this section we discuss the correlation between X-ray emission and density of galaxies as a function of the X-ray color.

The most widely used criteria to correlate two data sets are the *Pearson's correlation coefficient* r and the *Spearman's rank correlation coefficient* r_s (also known as *Spearman's rho*). Both assume values ranging from +1 (perfectly correlated) to -1 (completely anti-correlated). A null value means that the two quantities are not related at all. The first correlation coefficient is based on the assumption that the data follow a gaussian distribution, while the second makes no assumptions, measuring the correlation on ranked data (i.e. the data are converted to ranks and then correlated). The Spearman's rho is a better indicator that two variables are correlated when they are tied by a non-linear monotonous correlation.

In our case, cosmological models do not predict how galaxies and gas are linked. More specifically, it is not clear whether there is a linear correlation between density of galaxies and gas emission, or some physical mechanism links the formation of galaxies and the gas phase in a non-linear way. Therefore, the Spearman's rho is probably better suited in this

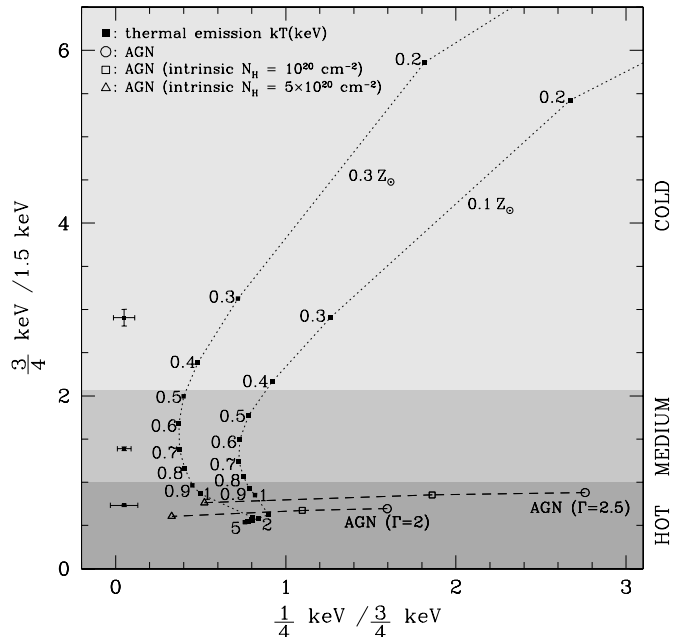


Figure 4. Color-color diagram ($[\frac{1}{4} \text{ keV}]/[\frac{3}{4} \text{ keV}]$ band ratio versus $[\frac{3}{4} \text{ keV}]/[1.5 \text{ keV}]$ band ratio) for various classes of sources. The dotted lines and full symbols indicate thermal emission (MEKAL model), corrected for Galactic absorption, at redshift $z = 0.1$ and metallicities $0.1 - 0.3 Z_{\odot}$, for several temperatures expressed in keV. The dashed lines and hollow symbols indicate colors of AGNs with two different slopes (quite typical in the *ROSAT* band), both unabsorbed and with intrinsic absorptions of $N_{\text{H}} = 1 - 5 \times 10^{20} \text{ cm}^{-2}$. The three horizontal shaded regions correspond to the three temperature bins adopted in Fig. 5 (for each of these regions the error on the average colors is shown). Note that plasmas with low temperatures ($kT < 0.5 \text{ keV}$) can be efficiently selected through high values of the $[\frac{3}{4} \text{ keV}]/[1.5 \text{ keV}]$ color (larger than ~ 2).

case. However, we will also show the Pearson's correlation results for comparison.

We do not expect to find a high correlation between galaxies and WHIM. In fact, the three *ROSAT* bands do not correlate strongly among themselves, with correlation coefficients in the range $0.2 \div 0.3$ (that means a low correlation).

Regions containing clusters would certainly give a higher value of r_s because they have lots of galaxies and high hard X-ray fluxes in small areas. Cooler regions should have few galaxies spread over large areas with low soft X-ray flux and therefore a low correlation signal is expected.

We have correlated the galaxy density map with the X-ray merged maps. Unfortunately, in this analysis we had to reject the 700528p field since it covers a region centered at the cross of 4 photographic plates of the Münster Survey, where the galaxy catalog shows clear spatial inhomogeneities. So we are left with the two deepest pointings with exposures greater than 19 ksec (fields 700133p-1 and 700275p). Moreover, since we use the ratio R45/R67 to discriminate between “cold” and “hot” regions, we selected those regions with a good signal in R45. In particular, we avoided exceedingly noisy regions by selecting the areas with the R45 flux higher than $M_X - 2\sigma_X$, where M_X is the me-

dian value and σ_X is the standard deviation over the field (anyhow this criterion selects most of the field, and more specifically ~ 95 per cent).

Fig. 5 shows the behavior of the correlation coefficient (Spearman’s rho and Pearson’s coefficients in upper and lower panels, respectively) as a function of the color [$\frac{3}{4}$ keV/1.5 keV] (R45/R67) for the three *ROSAT* energy bands. The temperatures corresponding to this ratio (assuming a metallicity of $0.3 Z_\odot$) are shown in the upper part of the graph and indicated in each plot by vertical dotted lines. The arrows show the position of the dotted lines in case of a metallicity of $0.1 Z_\odot$. We have measured the correlation for three temperature ranges to probe the “hot” ($kT > 0.9$ keV), “medium” ($0.5 - 0.9$ keV) and “cold” ($kT < 0.5$ keV) gas. For each range we show the median value of the R45/R67 ratio. Vertical error bars show the 1σ confidence on the value of the correlation coefficient.

The results from the two correlation coefficients do not differ significantly. The most important result is the finding of a weak, but significant correlation between the density of galaxy and the very soft $\frac{1}{4}$ keV flux, *only* for regions with gas temperature below 0.5 keV (i.e. “cold” regions). The correlation coefficient is 0.16–0.17 and significant at $3\sigma - 3.3\sigma$ (depending on the correlation coefficient adopted). The correlations with the other *ROSAT* bands (and other temperatures) do not show any significant signal, except for a marginal (2.5σ) correlation in the “hot” bin of the 1.5 keV band (which will be shortly discussed at the end of this section).

A correlation between galaxy distribution and very soft X-ray emission, limited to the “cold” ($kT < 0.5$ keV) regions, is just what is expected from WHIM emission which is tracing large-scale structures. However, there are a few other possibilities that could in principle explain the correlation in the soft band, as discussed in the following.

One alternative possibility is that the soft, cold emission is directly emitted by the individual galaxies of the SSC, or by a sub-population of them which are particularly active (starbursts). In this case the X-ray emission would be due to the warm-hot interstellar medium of the galaxies and to their superwinds. In our field there are at most 0.5 galaxy arcmin $^{-2}$. We have made two very conservative assumptions: 1) *all* these galaxies are starburst (and not dominated by a mixture of less active spirals and ellipticals); 2) the residual diffuse X-ray emission (due to Galactic Halo and extragalactic components) has the minimum value of 300×10^{-6} countss $^{-1}$ arcmin $^{-2}$ obtained by subtracting to the measured X-ray flux the *maximum* value of the LHB (see Section 4). We have assumed for a starburst a typical luminosity of 10^{41} erg s $^{-1}$ in the 0.5–2 keV energy band (see Figures 3-4 in Norman et al. 2004) and a spectrum made of a thermal component ($kT = 0.7$ and $Z = Z_\odot$) plus an absorbed power-law ($N_H = 10^{22}$ cm $^{-2}$ and $\Gamma = 0.8$) representing the X-ray binary contribution (see Norman et al. 2004). We have estimated that the galaxies should contribute a flux of $\sim 10^{39}$ erg s $^{-1}$ arcmin $^{-2}$ in the R2 *ROSAT* band. The latter value is a factor of ~ 20 lower than the average diffuse R2 flux of $\sim 10^{40.3}$ erg s $^{-1}$ arcmin $^{-2}$ that we measure in the *ROSAT* maps. This means that the X-ray emission from normal and starburst galaxies cannot contribute significantly to the correlation in the “cold” regions of the supercluster.

Another possibility, is that cold groups of galaxies could

contribute in some way to the correlation in the soft, cold regions. Indeed, a fraction of small groups may have temperatures as low as 0.4 keV (Mulchaey et al. 2003). However, as discussed in detail in the Appendix, the contribution to the coldest gas temperatures due to cold groups (i.e. those with $kT < 0.5$ keV) is at most the 1 per cent of the studied region. Therefore, “cold” groups cannot account for the soft X-ray emission nor for the correlation found in Fig. 4. Warmer systems, such as “hot” groups ($kT > 0.5$ keV) and clusters cannot explain the correlation; indeed these systems would give a significant correlation also in the higher temperature bins and also in the harder bands.

Finally, another possibility is that the correlation in the soft band, and at cold temperatures, is contributed by clusters/groups in formation and not yet virialized. These systems would have a temperature lower than standard clusters/groups. However, the distinction between forming, non virialized clusters/groups and WHIM is subtle, and probably just semantic. Indeed, the definition of WHIM (from a physical point of view) is that of a medium associated with forming, non-virialized structures (Cen & Ostriker 1999). Therefore, even a contribution from cold, forming clusters/groups should be included in the WHIM budget.

Summarizing, the scenario that better explains the correlation between galaxies and cold gas emitting at $\frac{1}{4}$ keV is that a fraction of the diffuse soft X-ray emission is due to WHIM associated with the galaxy distribution in the SSC.

In order to further investigate the latter scenario we have also tried to estimate the density of the emitting gas. Such estimate is very uncertain, since we do not have much information on the geometry of the emitting gas (the WHIM emission is disentangled only through a statistical analysis over a wide field). Moreover, we do not know exactly what fraction of the $\frac{1}{4}$ keV emission is actually emitted by the WHIM: indeed, although we measure a flux for the $\frac{1}{4}$ keV diffuse emission, the weak correlation with the galaxy distribution may either indicate a real, physically weak association between galaxies and WHIM, but may also point at a significant dilution from other unrelated X-ray components (foreground and background emission, Sect. 1). We have estimated the density of the gas emitting the soft X-ray radiation by making extreme, opposite assumptions on geometry of the gas (i.e. either distributed only in the putative filaments of Fig.2, or over the whole field where the cross-correlation was performed) and on its contribution to the $\frac{1}{4}$ keV emission (i.e. either contributing to the whole LHB-subtracted R2 emission, or only to the 20% responsible for the correlation with galaxies). The inferred gas densities range from 4×10^{-6} cm $^{-3}$ ($\delta \sim 15$), well in the range of the WHIM specifications, up to 10^{-4} cm $^{-3}$ ($\delta \sim 400$) which may be expected for WHIM in the proximity of clusters (Sect. 1).

Finally, we shortly discuss the nature of the marginal correlation between galaxy distribution and X-ray emission in the hard, R67 band (and some of R45), limited to “hot” temperatures (Fig. 5). This can be easily explained in terms of contribution from a population of unresolved, weakly obscured AGNs. Indeed, a small absorbing column density of $N_H \sim 0.5 - 1 \times 10^{21}$ cm $^{-2}$ is enough to absorb most of the $\frac{1}{4}$ keV flux, while leaving nearly unaffected the harder bands. Moreover, AGNs have R45/R67 colors nearly identical to “hot” plasma (see Fig. 4). Unresolved, obscured AGNs cer-

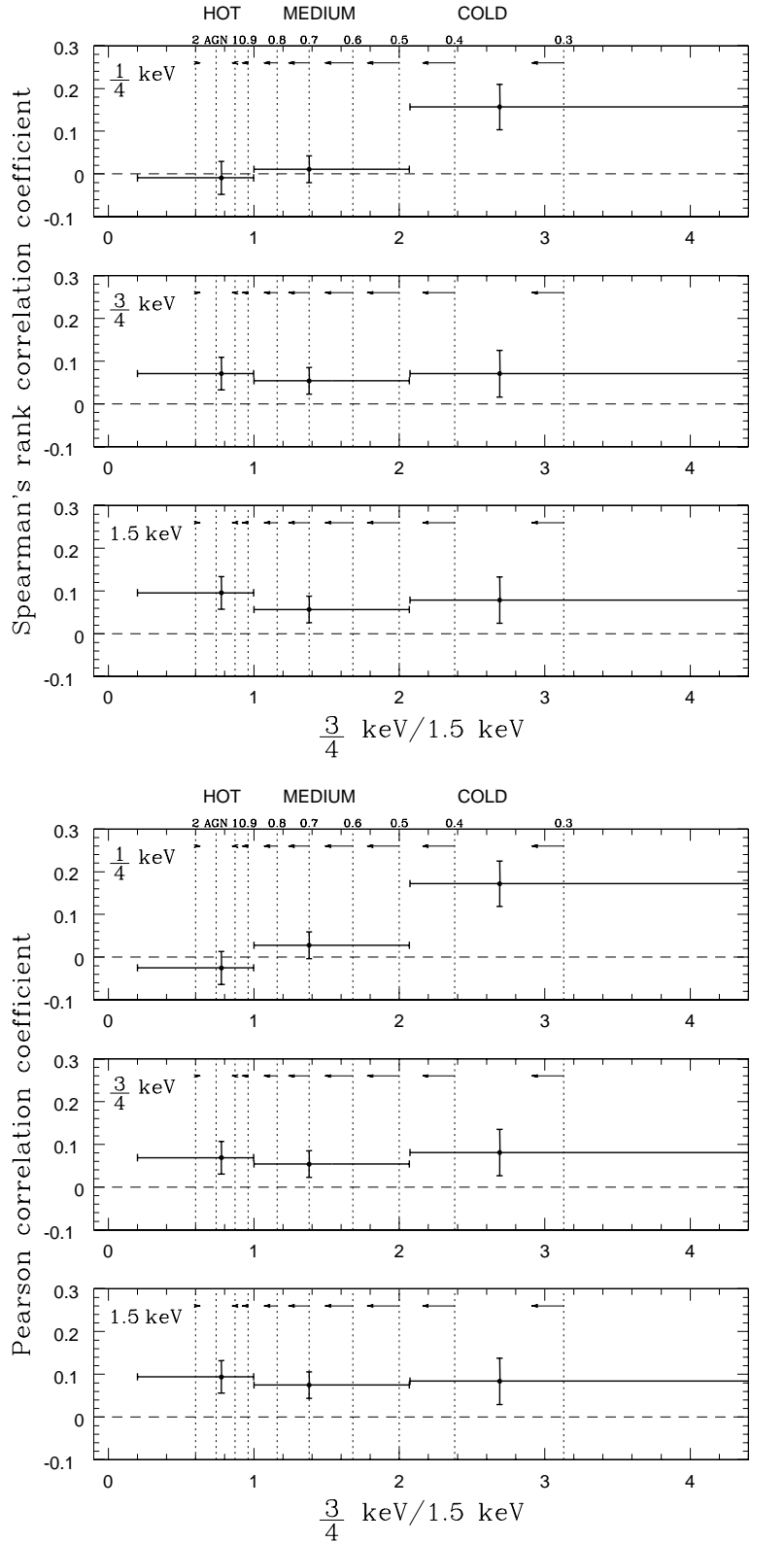


Figure 5. Correlation coefficient between galaxy distribution and X-ray emission, for the three ROSAT bands ($\frac{1}{4}$ keV, $\frac{3}{4}$ keV, 1.5 keV, from top to bottom), as a function of the $[\frac{3}{4}$ keV/1.5 keV] ratio. The vertical dotted lines indicate the plasma temperatures, as labelled at top of each panel, for a metallicity $0.3 Z_{\odot}$, corresponding to specific values of the $[\frac{3}{4}$ keV/1.5 keV] ratio. Arrows show the shift of the dotted lines in case of a metallicity of $0.1 Z_{\odot}$. The data are grouped in three main bins of temperature (“hot”, “medium” and “cold”). For each bin we indicate median value of the $[\frac{3}{4}$ keV/1.5 keV] ratio. The upper panel is for the Spearman’s correlation coefficient while the lower panel is for the Pearson’s correlation coefficient.

tainly contribute significantly to the X-ray background and span a wide range of absorbing N_H (Mainieri et al. 2002). Small amounts of X-ray absorption is also detected in several type 1 AGNs (Maiolino 2001; Maiolino et al. 2001) which are the dominant population found by *ROSAT* (Lehmann et al. 2001) and *Chandra* (Barger et al. 2003; Szokoly et al. 2004). Therefore, it is expected that a fraction (10-20 per cent) of unresolved AGNs which contribute to the diffuse signal detected by us are also slightly absorbed. These slightly obscured, unresolved AGNs (probably also belonging to the SSC) are probably responsible for the correlation in the hard band, and not in R2, for “hot” X-ray colors.

6 CONCLUSIONS

We have investigated the emission from Warm-Hot Inter-galactic Medium (WHIM) associated with large-scale structures in the central region of the Sculptor supercluster ($z \approx 0.1$). Ten overlapping *ROSAT* PSPC fields, covering the central 8.3×6.4 deg² of the supercluster, were analysed. After removal of the point sources, the *ROSAT* maps show indication of diffuse, filamentary structures, in some cases connecting known clusters of the Sculptor. The diffuse emission spans a wide range of X-ray spectral shapes: from relatively hard emission expected for clusters and unresolved AGNs, to very soft emission expected for WHIM.

To investigate the nature of the diffuse X-ray emission we have cross correlated the X-ray flux with the density of galaxies obtained from the Münster redshift catalog (whose galaxies mostly belong to the Sculptor supercluster in this region). The correlation has been analyzed as a function of the gas temperature (or X-ray spectral shape). The most important result is the finding of a significant correlation between the diffuse soft (0.1–0.3 keV) X-ray flux and the density of galaxies at the coolest gas temperatures ($kT < 0.5$ keV). Such a correlation is interpreted as emission by WHIM associated with the galaxy distribution.

We have also investigated the possible contribution to the diffuse soft X-ray emission, and to the correlation with galaxies, due to individual galaxies and by cold clusters. We have found that in both cases the contribution is negligible.

We have also detected a weak, marginal correlation between the harder X-ray flux (1.5 keV, R67 band) and the density of galaxies at apparently higher gas temperatures ($kT \sim 1$ keV). The latter correlation is ascribed to slightly obscured, unresolved AGNs.

ACKNOWLEDGEMENTS

We thank the referee, F. Nicastro for his comments and helpful suggestions. We are also grateful to A. Ferrara for very useful comments. This work was partially supported by the Italian Ministry of Research (MIUR) and by the Italian Institute of Astrophysics (INAF).

APPENDIX A: THE CONTRIBUTION FROM COLD GROUPS OF GALAXIES

Groups of galaxies are poorly studied objects because of their elusive nature both in the X-rays and optical. One

of the largest samples studied so far (Mulchaey et al. 2003) contains 109 low-redshift galaxy groups. It is a collection of several catalogs of groups selected both in X-ray and optical. In this catalog temperatures have been derived only for a subsample of 61 objects that show also extended diffuse emission. The temperatures derived for these clumps range from 1.5 keV down to 0.4 keV. The latter overlaps the range of WHIM temperatures. As a consequence, “cold” groups could mimic the WHIM behavior, both in terms of X-ray spectral shape and correlation with galaxies. Therefore, it is important to quantify the density of “cold” clusters and to estimate their contribution to the soft X-ray emission. The coldest groups ($kT < 0.5$ keV) are also the smallest ($R_X < 120$ kpc) and the least luminous ($L_X < 10^{41.2}$ erg/s). To calculate the fraction of area expected to be covered by groups we have used the catalog of groups detected by the ESO Slice Project (ESP; Ramella et al. 1999) in a field close to the SSC region (~ 10 deg away). The survey has been done in two strips. We consider only the area near to the SSC (strip A; 22×1 deg). In this region they found 190 groups up to redshift $z = 0.2$, ~ 71 at redshifts below the z_{SSC} , and only 18 below $z = 0.05$. We can assume the extreme scenario that all groups are colder than 0.5 keV and that all of them have a size $R_X \sim 120$ kpc (which is the maximum size found among cold groups). With these assumptions, we can calculate what is the maximum fraction of our field occupied by cold groups in the following redshift ranges: 0–0.05, 0.05– z_{SSC} , z_{SSC} –0.2. To make things simpler we calculate the angular sizes of groups in these bins using the mean redshift value, except for the last one where we assume that all groups have redshift z_{SSC} . We exclude from the sample all the identified groups with 3 galaxy members because almost all these groups do not show diffuse emission that can contribute to the correlations (Mulchaey et al. 2003). With these extreme, conservative assumptions we obtain that at most 1 per cent of the pixels in our image could be significantly contaminated by cold groups emission. This means that cold groups cannot contribute to the correlation found in regions with $kT < 0.5$ keV.

REFERENCES

- Bagchi J., EnBlin T. A., Miniati F., Stalin C. S., Singh M., Raychaudhury S., Humeshkar N. B., 2002, *New Astronomy*, 7, 249
- Barger A. J., Cowie L. L., Capak P., Alexander D. M., Bauer F. E., et al., 2003, *AJ*, 126, 632
- Bertin E., Arnouts S., 1996, *A&AS*, 117, 393
- Bregman J. N., Irwin J. A., 2002, *ApJ*, 565, L13
- Cen R., Kang H., Ostriker J. P., Ryu D., 1995, *ApJ*, 451, 436
- Cen R., Ostriker J. P., 1999, *ApJ*, 514, 1
- Croft R. A. C., Di Matteo T., Davé R., Hernquist L., Katz N., et al., 2001, *ApJ*, 557, 67
- Davé R., Cen R., Ostriker J. P., Bryan G. L., Hernquist L., et al., 2001, *ApJ*, 552, 473
- Einasto M., Tago E., Jaaniste J., Einasto J., Andernach H., 1997, *A&AS*, 123, 119
- Fang T., Croft R. A. C., Sanders W. T., Houck J., Davé R., et al., 2004, *ApJ* submitted, astro-ph/0311141

- Finoguenov A., Briel U. G., Henry J. P., 2003, *A&A*, 410, 777
- Fukugita M., Peebles P. J. E., 2004, astro-ph/0406095
- Hellsten U., Gnedin N. Y., Miralda-Escudé J., 1998, *ApJ*, 509, 56
- Kaastra J. S., Lieu R., Tamura T., Paerels F. B. S., den Herder J. W., 2003, *A&A*, 397, 445
- Kuntz K. D., Snowden S. L., Mushotzky R. F., 2001, *ApJ*, 548, L119
- Lehmann I., Hasinger G., Schmidt M., Giacconi R., Trümper J., et al., 2001, *A&A*, 371, 833
- Mainieri V., Bergeron J., Hasinger G., Lehmann I., Rosati P., et al., 2002, *A&A*, 393, 425
- Maiolino R., 2001, in *AIP Conf. Proc.* 599: X-ray Astronomy: Stellar Endpoints, AGN, and the Diffuse X-ray Background Obscured active galactic nuclei. pp 199–208
- Maiolino R., Marconi A., Salvati M., Risaliti G., Severgnini P., et al., 2001, *A&A*, 365, 28
- Mathur S., Weinberg D. H., Chen X., 2003, *ApJ*, 582, 82
- Mulchaey J. S., Davis D. S., Mushotzky R. F., Burstein D., 2003, *ApJS*, 145, 39
- Nicastro F., Zezas A., Drake J., Elvis M., Fiore F., et al., 2002, *ApJ*, 573, 157
- Norman C., Ptak A., Hornschemeier A., Hasinger G., Bergeron J., et al., 2004, *ApJ*, 607, 721
- Obayashi H., Makishima K., Tamura T., 2000, *Advances in Space Research*, 25, 625
- Perna R., Loeb A., 1998, *ApJ*, 503, L135
- Pierre M., Bryan G., Gastaud R., 2000, *A&A*, 356, 403
- Ramella M., Zamorani G., Zucca E. et al. and Stirpe G. M., Vettolani G., et al., 1999, *A&A*, 342, 1
- Scharf C., Donahue M., Voit G. M., Rosati P., Postman M., 2000, *ApJ*, 528, L73
- Schuecker P., Ott H., 1991, *ApJ*, 378, L1
- Seitter W. C., 1992, in MacGillivray H. T., E.B. T., eds, *Digitised Optical Sky Surveys Digitised Optical Sky Surveys*. Kluwer Academic Publishers, pp 321–324
- Snowden S. L., Freyberg M. J., Kuntz K. D., Sanders W. T., 2000, *A&AS*, 128, 171
- Snowden S. L., McCammon D., Burrows D. N., Mendenhall J. A., 1994, *ApJ*, 424, 714
- Sołtan A. M., Freyberg M. J., Hasinger G., 2002, *A&A*, 395, 475
- Spiekermann G., 1996, in *Roentgenstrahlung from the Universe The Sculptor Supercluster at z=0.11 – Investigation with ROSAT and the ESO/SERC IIIa-F Survey*. pp 615–616
- Spiekermann G., Seitter W. C., Boschan P., Cunow B., Duemmler R., Naumann M., Ott H.-A., Schuecker P., Ungruhe R., 1994, *Reviews of Modern Astronomy*, 7, 207
- Szkody G. P., Bergeron J., Hasinger G., Lehmann I., Kewley L., et al., 2004, *ApJS* in press, astro-ph/0312324
- Tittley E. R., Henriksen M., 2001, *ApJ*, 563, 673
- Tripp T. M., 2002, in *ASP Conf. Ser.* 254: Extragalactic Gas at Low Redshift Highly-Ionized Intergalactic Gas at Low Redshifts: Constraints from QSO Absorption Lines. p. 323
- Ungruhe R., 1999, PhD thesis, University Münster
- Ungruhe R., Seitter W. C., Duerbeck H. W., 2003, *Journal of Astronomical Data*, 9, 1
- Vikhlinin A., McNamara B. R., Forman W., Jones C., Quintana H., Hornstrup A., 1998, *ApJ*, 502, 558
- Yoshikawa K., Yamasaki N. Y., Suto Y., Ohashi T., Mitsuda K., et al., 2003, *PASJ*, 55, 879
- Zappacosta L., Mannucci F., Maiolino R., Gilli R., Ferrara A., Finoguenov A., Nagar N. M., Axon D. J., 2002, *A&A*, 394, 7